Study of Behavior of Reinforced Concrete Beams with Smart Rebars Using Finite Element Modeling

A. R. Khaloo[1,*],I. Eshghi[2] and P. Piran Aghl[2]

Received: October 2009 Accepted: August 2010

Abstract: *In this paper the response of cantilevered reinforced concrete (RC) beams with smart rebars under static lateral loading has been numerically studied, using Finite Element Method. The material used in this study is SuperelasticShape Memory Alloys (SE SMAs) which contains nickel and titanium elements. The SE SMA is a unique alloy that has the ability to undergo large deformations and return to their undeformed shape by removal of stresses. In this study, different quantities of steel and smart rebars have been used for reinforcement andthe behavior of these models under lateral loading, including their load-displacement curves, residual displacements, and stiffness, were discussed. During lateral loading, rebars yield or concrete crushes in compression zone in some parts of the beams and also residual deflections are created in the structure. It is found that by using SMA rebars in RC beams, these materials tend to return to the previous state (zero strain), so they reduce the permanent deformations and also in turn create forces known as recovery forces in the structure which lead into closing of concrete cracks in tensile zone. This ability makes special structures to maintain their serviceability even after a strong earthquake.*

Keywords: *Shape Memory Alloy, Reinforced Concrete Beam, Smart Rebar, Residual Displacement, Lateral Stiffness*

1. Introduction

In recent years, the dream of designing and constructing smart structures is becoming a reality. Civil engineers with the help of metallurgical science have created innovative structural materials which can display predetermined physical characteristics.

Shape Memory Alloys (SMAs) are a novel functional material which can exhibit little residual strains under cycles of loading and unloading even after passing the yielding zone. They have the ability to remember a predetermined shape even after severe deformations which enable them to be widely used in numerous applications in the area of 'smart materials' or 'intelligent materials' [1-10].

In 1965, shape memory alloys (Nitinol) which derived from Nickel and Titanium were first patented by Buehler and Wiley [11] in Naval Ordnance Laboratory. Depending on the temperature, SMA can be austenite, martensite or the mixture of them. Indeed, these alloys are particularly useful when large deformation and recovery of the shape is observed under a small rate of stress or temperature.

In recent years, the two major properties of SMAs have attracted the attention of many researches for application to smart structural systems. One is the shape memory effect (SME), in which a specimen exhibits a larger residual strain after loading and unloading that can be fully recovered upon raising the temperature of the material. This recovery stress can be used for introducing forces in structures. The other important phenomenon is the superelastic effect (SE), in which a specimen achieves a very large strain by the phase transformation from austenite to martensite upon loading that is then fully recovered in a hysteresis loop upon unloading and without thechanging the temperature. Besides, both SME and SE are caused by phase transformation.

One of the recent researches have been done by Saiidi and Wang [12] on seismic response of concretecolumns with SMAs reinforcement which investigates the effectiveness of these materials to reduce the residual displacements of columns. Moreover, Saiidi et al. [13] investigated the effectiveness of Superelastic SMA simply supported RC beams in reducing permanent deformation where SMA was used as tensile

* *Corresponding author. Email: khaloo@sharif.edu*

1, Professor of Structural Engineering, Sharif University of Technology, Tehran.*

2 M.Sc in Earthquake Engineering, Sharif University of Technology, Tehran.

reinforcement only at the critical region of the beam.Li et al. [14] have studied the behavior of a simple concrete beam driven by heated SMA wires using electrical currents.Also the investigation ofCzaderski et al. [15] shows that by using the constrained recovery effect, it is possible to produce a changeable prestress in the RC beam.

In the present study, finite element analysis of reinforced concrete beams using smart rebar were performed to investigate the effect of ratio of SMArebars, loading amplitude, and strength of concrete on the behavior of RC beams embedded with SMA wires. At first, both characteristics of materials and finite element model are described. Then, results of analysis using ANSYS software are presented and discussed. At the end, a parametric study is performed to study the influence of different parameters on the cyclic response of RC beams.

2. Characteristics of Materials

2.1. Concrete

The modeling of concrete considers cracking, crushing failure modes and nonlinear behavior.The compressive strength of concrete is 30 MPa and its tensile strength is 3.5 MPa. Also the elastic modulus and poisson's ratio are 20 GPa and 0.2, respectively. The concrete material model in the ANSYS software predicts the failure of brittle materials by using the model of Willam and Warnke [16].

2.2. Steel

Bilinear stress-strain curve has been used for the modeling of steel behavior. The values of elastic modulus and poisson's ratio of steel are 200 GPa and 0.3, respectively.

The model, which introduces the behavior of steel in nonlinear form, is based on the model of Bilinear Kinematic Hardening. The steel is assumed to have yield strength of 400 MPa.

2.3. Shape Memory Alloys

In order to modelSMA in ANSYS software, the predetermined nonlinear model, which is provided in material library, has been used here. This model is used for describing the superelastic effect of NiTi-based alloys as well. The term SE refers to a recovery of the large deformations in loading-unloading cycles, occurring at the certain temperatures. Furthermore, the capability of these classes of materials in recovering the possible accumulated deformations by heat treatment is called SME.

SMAs are found in two main phases: the high temperature phase, which is called austenite, and the low temperature phase, which is called martensite. Besides, these types of materials could be transformed from austenite to martensite either by reducing the temperature or by applying a mechanical stress [17].

Figure 1 shows the stress-strain relationship for the SMA which has been used in ANSYS software. In this figure, σ_s^{AM} and σ_f^{AM} are starting and final stresses for the forward transformation (austenite to martensite) respectively, σ_s^{MA} and σ_f^{MA} are starting and final stresses for the reverse transformation (martensite to austenite) respectively, E_A is the elastic modulus of the austenite phase, and $_L$ is the maximum residual phase. The values of these parameters are also listed in table 1.

An experimental study presented by Auricchio and Sacco [17, 18] was used here due to obtaining the starting and final stresses, and the elastic modulus of SMA.This type of material is manufactured by Nitinol Devices & Components (NDC) which is one of the most common types of SMA.Additionally, the SMA modeling in ANSYS software is based on Auricchio model.

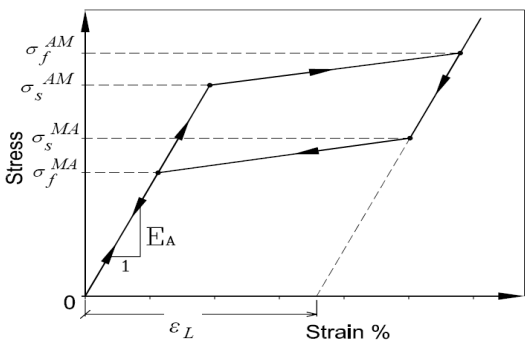

Fig. 1. Stress-strain curve for SMA.

3.1. Geometrical Modeling

The concrete beam has a length of 2 m and is rectangular in cross section with dimensions of 340 mm by 280 mm. Owing to studying the effect of different quantities of steel and smart rebar, the width of the cross section has been assigned longer than its height to place more longitudinal rebar.

Table 1. Parameters of the stress-strain curve for SMA.

Parameter	Value
σ_s^{AM}	520 MPa
σ_f^{AM}	600 MPa
σ_s^{MA}	240 MPa
σ_f^{MA}	200 MPa
E_A	60 GPa
$\bar{e}_L$	8%

3. Characteristics of Finite Element Model

Regarding concrete model meshes, it is noticeable that by using SOLID 65 element the nonlinear behavior and also the capability of cracking and crushing of the concrete have been considered. In ANSYS software, SMAs can be specified for the following elements: PLANE182, PLANE183, SOLID185, SOLID186, SOLID187, and SOLSH190 [19]. The most suitable elements for 3-D rebar modeling are SOLID elements. Besides, the number of node and order are the same in both elements SOLID185 and SOLID 65; both SOLID185 and LINK8 can be used to 3-D modeling. Since the details of both SMA and steel reinforcement must be changed frequently, using SOLID185 element for the entire reinforcements provides high speed during modeling process.LINK8 element has been used here for stirrups modeling of concrete beam.

Hexahedral-shaped elements have been used to mesh the model. Each element has the dimensions of 2×2×4 cm^3. Due to having a uniform meshing in cross section, width and height of the beam cross section has been divided into 17 and 14 equal pieces. In this way, the cross section of the concrete beam has a regular meshing area with the dimensions of 2×2 cm^2. Besides, the length of the beam has been divided into 50 pieces of equal length.

3.2. Details of Reinforcement

Assuming 6% reinforcement ratio, 14 rebars with 4 cm^2 of cross sectional area is used to reinforce the beam. Although this amount of ratio is the upper limit, the purpose of this study is to investigate the influence of the smart rebars on the concrete beam behavior. Hence, this amount of ratio and various arrangements of reinforcement make it possible to compare the effect of smart rebars to that of steel rebarsin behavior of concrete beam. As described further in the paper, the width of the cross section is longer than its height in order to place more longitudinal rebars. Ratio of smart rebars to total bars for five different arrangements of reinforcement are shown in table 2. The section of beam for each arrangement is also shown in figure 2.

In order to confine the concrete, maximum amount of shear reinforcement has been used for stirrup modeling which prevents brittle shear failure [20]. The width and the effective depth of the beam section were set to 340 mm and 230 mm, respectively. By using closed stirrups at 40 mm centers, the calculated value for the area of stirrups is 62 mm^2.

3.3. Loading and Boundary Conditions

In this paper, response of a cantileveredbeam is studied under cyclic lateral loading. The lateral load was applied to the end of the beam in X direction, as shown in figure 3.

Loading process was carried out based on displacement control with the maximum displacement of 0.15 m. Figure 4 shows the displacement-time relationship for the concrete beam.

Table 2. Ratio of smart rebars.

No. of smart rebars	Ratio of smart rebar to total bars
0	R= 0.00
2	R= 0.14
4	R= 0.29
6	R= 0.43
8	R= 0.57

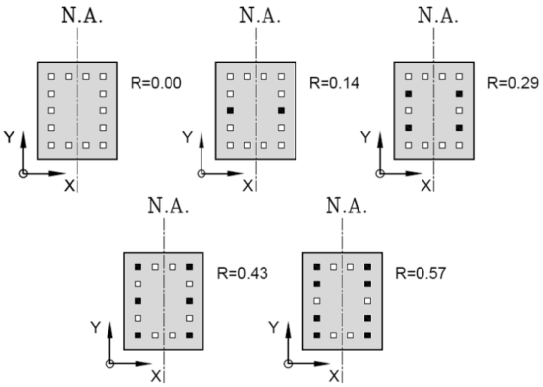

Fig. 2. Arrangements of longitudinal reinforcement in section of beam.

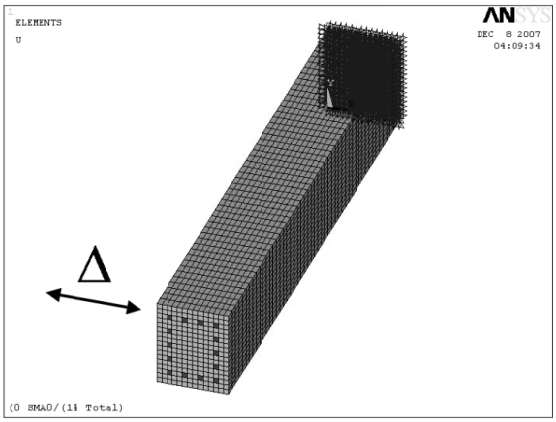

Fig. 3. Direction of lateral loading.

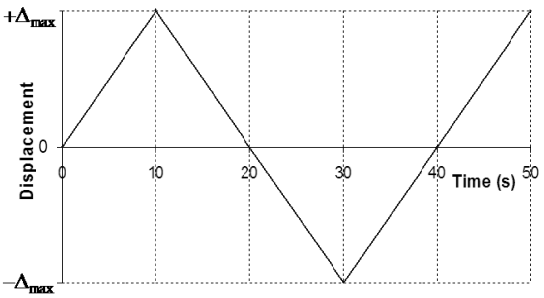

Fig. 4. Displacement-time relationship for the end of concrete beam.

3.4. Analysis Method

The behavior of beam has been studied here by the use of nonlinear static analysis in largedisplacementcondition. Due to controlling the convergence ……at every performance of analysis at every substep, both force and displacement convergence criteria have been

convergence

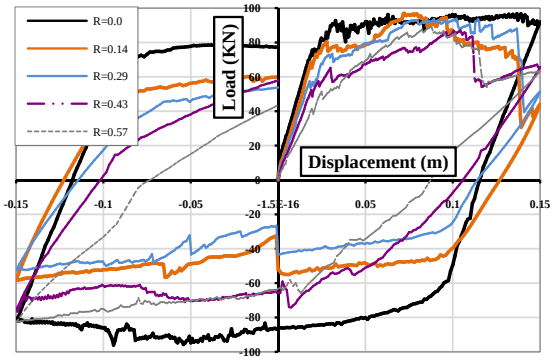

Fig. 5. Hysteresis curve of shear force versus displacement for models.

performed by using the tolerance value of 0.01.The maximum number of iteration in each substep is 120.

4. Results of Analysis

In this section, the results of the numerical study of the concrete beam models have been presented. The results due to the various details of smart rebars have been compared as well.

4.1. Load-DispLacement Diagrams

Figure 5 shows hysteresis curve of shear force vs. displacement for concrete beam. The displacement of the models is measured at the end of the concrete beam. This figure indicates that increase in the ratio of smart rebar, reduces the area of the hysteresis P-Ä curves. This is due to smaller area under stress-strain curve of smart rebar compared to that of ordinary reinforcement.

Figure 6 (a) and (b) illustrates the stress-strain curve for steel rebar and smart one, respectively. These curves are obtained from the elements near the constrained region ofbeam. Due to concrete compressive response, there is less compressive strain in SMA (figure 6(b)).

4.2. Residual Displacement

Residual displacements of the models are given in table 3. Smart rebars reduces residual displacement. In the third column of this table, reduction of residual displacement due to SMA to that of without SMA is expressed as a percentage.

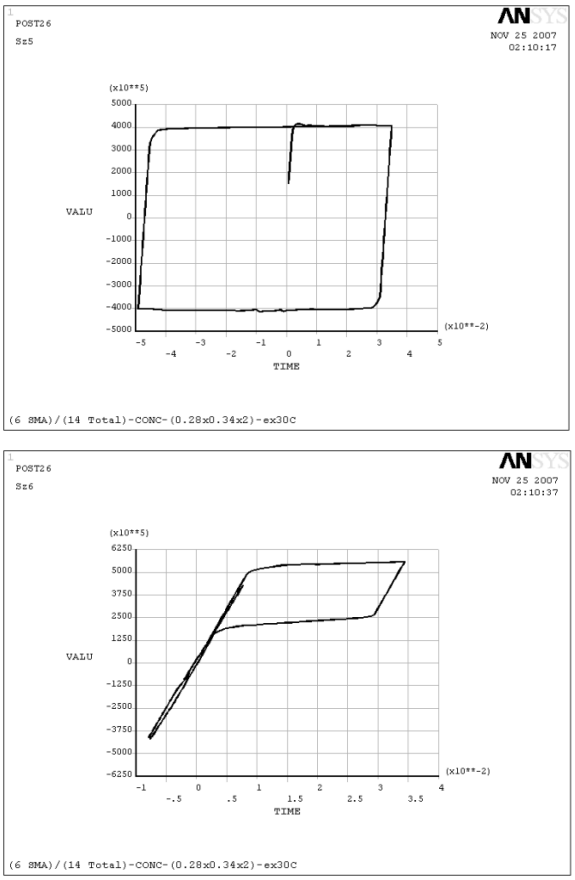

Fig. 6. Stress-strain curve: (a) steel rebar, (b) smart rebar.

Table 3. Residual displacement of the models.

Ratio of smart rebar	Residual displacement (cm)	Reduction of residual displacement (%)
0.00	11.67	0.00
0.14	10.81	7.35
0.29	10.10	13.43
0.43	8.75	25.04
0.57	6.45	44.69

For higher ratio of smart rebars, higher residual displacement is reduced. At the end of the loading, SMA rebars tend to return to the zero strain. Therefore, they create recovery forces which lead into both closing of concrete cracks and reduction of residual displacement.

4.3. Stiffness

The stiffness of the cantilevered beam before cracking can be obtained by use of material strength formula ($K=3EI/L^3$). The equivalent section of the beam has been used to obtain the parameters I and E. Table 4 contains the stiffness of the models for each ratio of smart rebar. According to this table, smart rebar causes reduction of stiffness inbeam before cracking and higher ratio of smart rebar provides higher percentage in stiffness reduction. Since the elastic modulus of SMA is much less than that of steel, both modulus of equivalent section and stiffness decreased by replacing steel with smart rebars. In fact, smaller amount of elastic modulus of SMA than steel (60 GPa vs. 200 GPa) is a

Table 4. Section modulus and lateral stiffness of the models.

Ratio of smart rebar(R)	I (cm^4)	K (KN/m)	Percentage of stiffness reduction (%)
0	92653	6949	0.0
0.14	88117	6609	4.9
0.29	83581	6269	9.8
0.43	79045	5928	14.7
0.57	74509	5588	19.6

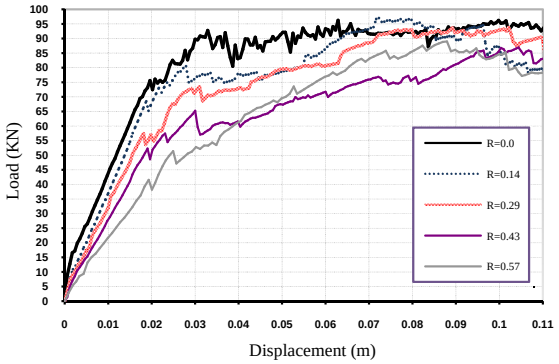

Fig. 7. Load-displacement curves of the models.

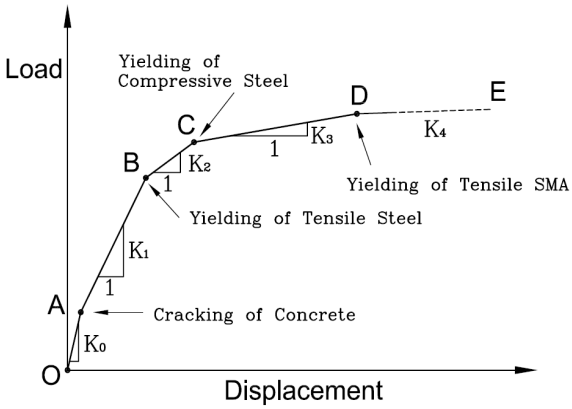

Fig. 8. Schematic curve of lateral load versus displacement.

disadvantage of these materials in addition to its relatively high price.

The slope of load-displacement curve has been used as the lateral stiffness of the models after cracking. Figure 7 shows load-displacement curves of the models for displacement up to 0.11 m.

Each curve of the models is divided into four zones. Schematic diagram of the load-displacement relationship for the beam is presented in figure 8.

In OA zone, the behavior of beam is elastic and also there is no crack in the concrete section. Point A illustrates the beginning of cracking in the tension area. In AB zone, the concrete cracks appear beneath the neutral axis;however the behavior of the all reinforcements remained elastic. Tension steel rebars yield at point B and compression steel rebars yield at point C, however the elastic behavior of the smart rebars remain. Eventually, tension smart rebars yield at point D. In all of the models it is noticeablethat none of the smart rebarstrains has reached yield strainin the compression area and has remained elastic.

The stiffness of the beam before cracking, which is denoted by K_0, studied at the beginning of this section. It is evident from figure 7 that increase in the ratio of smart rebar reduces the lateral stiffness of the beam in zone AB and BC. Since all of the steel rebars have not yielded in these two zones and also elastic modulus of steel rebar is much higher than that of smart rebar, the stiffness of the models is higher for cases with higher steel content. Due to yielding of thetension steel rebar in BC zone, variations in the beam stiffness of BC zone is less than that of AB zone.

In zone CD, the increase in the ratio of smart rebar increases lateral stiffness of the beam which is denoted by K_3. In this zone steel reinforcement yields and has no stiffness while smart rebar is still in the elastic range.

Table 5. Models with various values of R and E.

Ratio of smart rebar	Test number of models			
	$E=0.1E_c$ (2GPa)	$E=0.3E_c$ (6GPa)	$E=0.5E_c$ (10GPa)	$E=0.7E_c$ (14GPa)
R=0.0	7	12	17	22
R=0.14	8	13	18	23
R=0.29	9	14	19	24
R=0.43	10	15	20	25
R=0.57	11	16	21	26

5. Parametric Study

Three variables have been considered for parametric study. The variables are loading amplitude (level of beam tip displacement), ratio of smart rebar, and strength of concrete, and there are 4, 5, and 4 different values for each of parameters respectively. Consequently, in total 80 models are evaluated.

5.1. Loading Amplitude

Lateral loading is displacement controlled (refer to figure 4). Four levels are considered for the maximum displacement of the beam (Δ_{max}) as given below:

- A series models (Δ_{max}=0.25m)
- B series models (Δ_{max}=0.20m)
- C series models (Δ_{max}=0.15m)
- D series models (Δ_{max}=0.10m)

The main target is to investigate the effect of loading amplitude on the performance of smart rebar for reducing residual displacement.

5.2. Ratio of Smart Rebars

The ratios of the smart rebars are the same as that in table 1. The test number of models related to each ratio is listed in table 5.

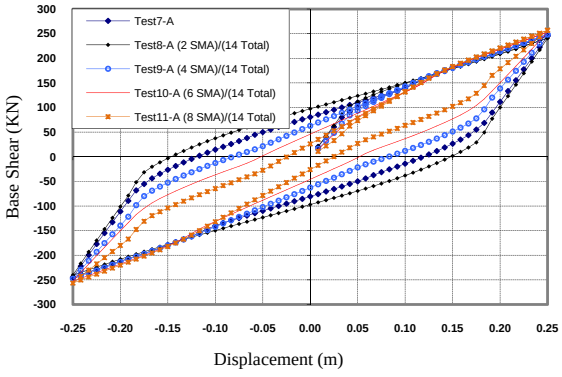

Fig. 9. Base shear-displacement for Δ_{max}=0.25m and E=0.1Ec.

5.3. Strength of Concrete

An elastic material with young's modulus lower than concrete is used to eliminate the influence of cracking and crushing on the beam response. Indeed, crackedconcrete is replaced with a material of low young's modulus which allows studying large displacement. Four young's moduli are used to investigate the effect of concrete strength on the behavior of beam (figure 5). Results of the analysis of this material contrast with that of real one. However, according to the next section the effect of smart rebars on the concrete models with the low young's modulus is quite similar to the effect of that on the real concrete models which have the capability of cracking and crushing.

6. Results of Parametric Study

The effect of different variables on load-displacement curve, residual displacement, and stiffness of the models are discussed below.

6.1. Load-Displacement Curves

Figure 9 plots base shear versus displacement at the end of the beam for Δ_{max}=0.25m and E=0.1E_c.

This diagram has been plotted for all of the values Ämaxand E, however, a typical response is shown here. Comparing these diagrams indicates that replacing steel bars with SMA bars reduces the area of the hysteresis P-Δ curves. Besides, it reduces energy absorption capacity of the concrete beam due to the difference between the stress-strain curve of SMA and that of steel (figure10). These curves are obtained through the analysis of the elements next to the fixed end of the 9-A model.

Since SMAs have the properties of SE and SME, they have little residual strain and also the area under the stress-strain curve for SMA is much lower than that of steel. In view of this reason, replacing steel bars with SMA bars contributes to reducing the energy absorption capacity of the structures.

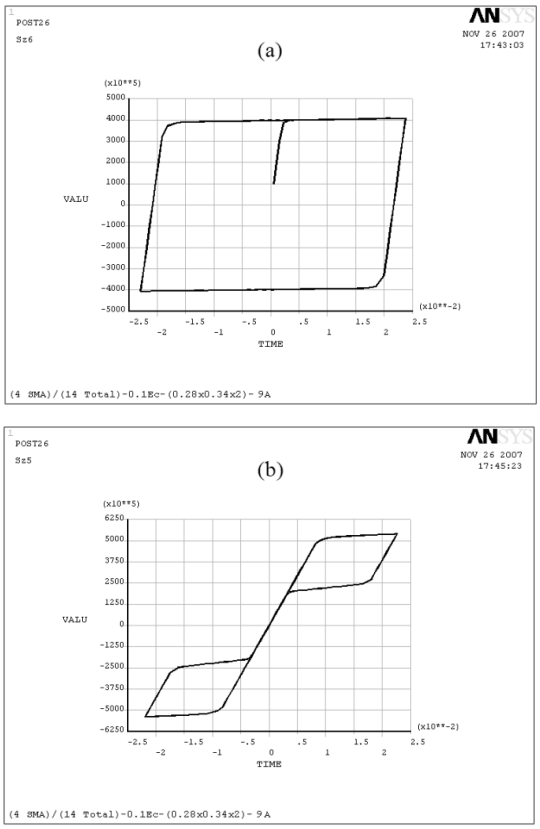

Fig. 10. Stress-strain curve for 9-A model: (a) steel rebar, (b) smart rebar.

6.2. Residual Displacement

Table 6 presents the properties of the models and their residual displacements. For each model with certain value of young' modulus and specific loading amplitude, the reduction of residual displacement has been calculated as a percentage of residual displacement of the model without SMA rebars.

Figure 11 shows the reduction of residual displacement due to ratio of smart rebar. There are four diagrams which have different values of the concrete strength. The strength of concrete is constant and the load amplitude is variable for each diagram.

The diagrams indicate following results.

- Diagram A: for a certain value of the ratio of smart rebars, higher maximum displacement yields higher reduction of residual displacement. On the other hand,

for the concrete with low strength, the higher loading amplitude results in more effective force recovery of smart rebar.

- Diagram B: the effect of both loading amplitude and reduction of residual displacement decrease, due to increase in the elastic modulus to $0.3E_c$, except for the case of Δ_{max}=0.1m due to the elastic behavior of SMA.
- Diagram C: the loading amplitude does not affect the reduction of residual displacement, except the case of Δ_{max}=0.1m, as expected. However, the differences are insignificant.
- Diagram D: by increasing the elastic

Table 6. Residual displacement of models in parametric study.

Concrete young's modulus	R	Δ_{max}=0.25m Residual dis. (cm)	Δ_{max}=0.25m Reduction of residual dis. (%)	Test No.	Δ_{max}=0.2m Residual dis. (cm)	Δ_{max}=0.2m Reduction of residual dis. (%)	Test No.	Δ_{max}=0.15m Residual dis. (cm)	Δ_{max}=0.15m Reduction of residual dis. (%)	Test No.	Δ_{max}=0.1m Residual dis. (cm)	Δ_{max}=0.1m Reduction of residual dis. (%)	Test No.
	0.00	14.79	0.0	7-A	12.20	0.0	7-B	8.65	0.0	7-C	4.65	0.0	7-D
	0.14	11.84	20.0	8-A	9.97	18.3	8-B	7.56	12.6	8-C	4.13	11.2	8-D
$0.1E_c$	0.29	8.26	44.2	9-A	7.13	41.5	9-B	5.62	35.0	9-C	3.47	25.4	9-D
	0.43	4.81	67.5	10-A	4.37	64.2	10-B	3.65	57.8	10-C	2.52	45.8	10-D
	0.57	2.60	82.4	11-A	2.35	80.7	11-B	1.91	77.9	11-C	1.32	71.6	11-D
	0.00	7.08	0.0	12-A	6.42	0.0	12-B	5.37	0.0	12-C	3.53	0.0	12-D
	0.14	5.43	23.3	13-A	4.98	22.4	13-B	4.24	21.0	13-C	2.96	16.0	13-D
$0.3E_c$	0.29	3.97	43.9	14-A	3.66	42.9	14-B	3.15	41.3	14-C	2.29	35.0	14-D
	0.43	2.68	62.1	15-A	2.47	61.5	15-B	2.11	60.7	15-C	1.56	55.7	15-D
	0.57	1.53	78.4	16-A	1.38	78.6	16-B	1.12	79.1	16-C	0.80	77.3	16-D
	0.00	4.56	0.0	17-A	4.23	0.0	17-B	3.68	0.0	17-C	2.66	0.0	17-D
	0.14	3.58	21.4	18-A	3.34	21.2	18-B	2.92	20.7	18-C	2.17	18.5	18-D
$0.5E_c$	0.29	2.68	41.3	19-A	2.49	41.1	19-B	2.18	40.7	19-C	1.65	37.9	19-D
	0.43	1.85	59.4	20-A	1.71	59.7	20-B	1.47	60.0	20-C	1.12	58.1	20-D
	0.57	1.08	76.3	21-A	0.97	77.1	21-B	0.79	78.4	21-C	0.57	78.6	21-D
	0.00	3.36	0.0	22-A	3.15	0.0	22-B	2.78	0.0	22-C	2.10	0.0	22-D
	0.14	2.67	20.4	23-A	2.50	20.5	23-B	2.21	20.4	23-C	1.70	19.1	23-D
$0.7E_c$	0.29	2.02	39.8	24-A	1.89	40.0	24-B	1.66	40.2	24-C	1.29	38.7	24-D
	0.43	1.41	57.8	25-A	1.31	58.5	25-B	1.13	59.4	25-C	0.87	58.7	25-D
	0.57	0.84	75.1	26-A	0.75	76.2	26-B	0.61	78.0	26-C	0.44	78.9	26-D

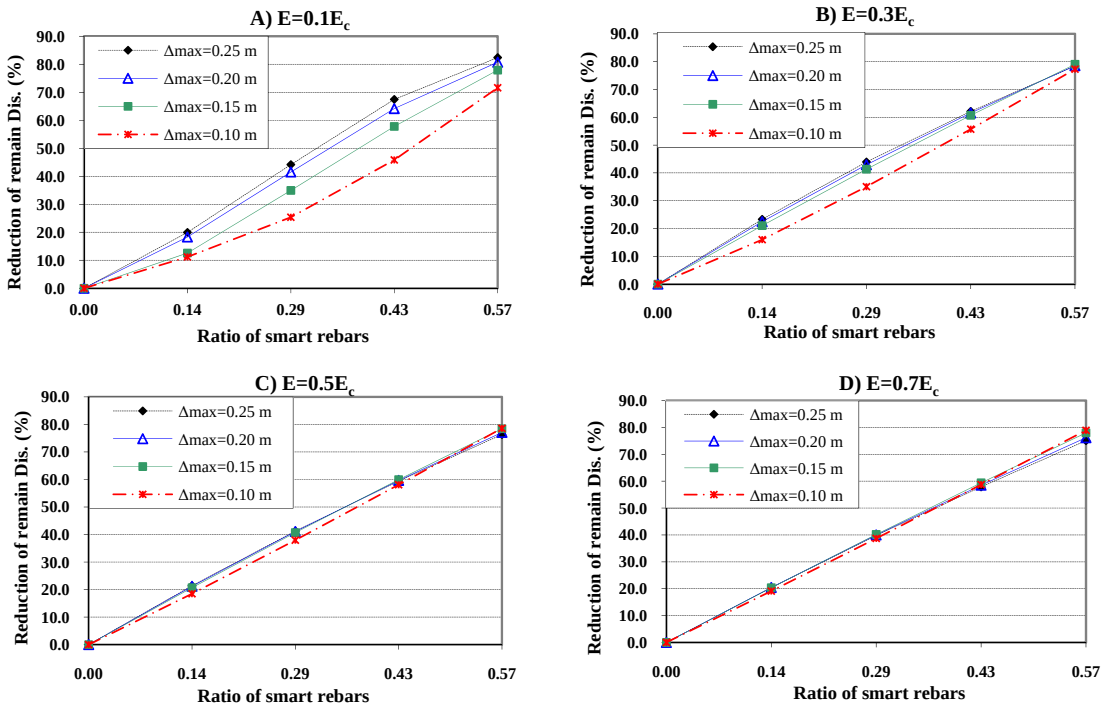

Fig. 11. Relationship between reduction of residual displacement and ratio of smart rebar.

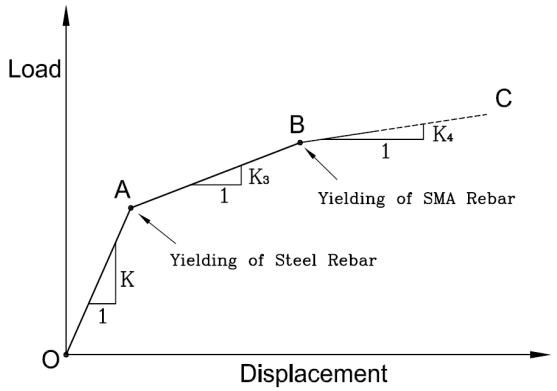

Fig. 12. Schematic curve of load versus displacement for the elastic models.

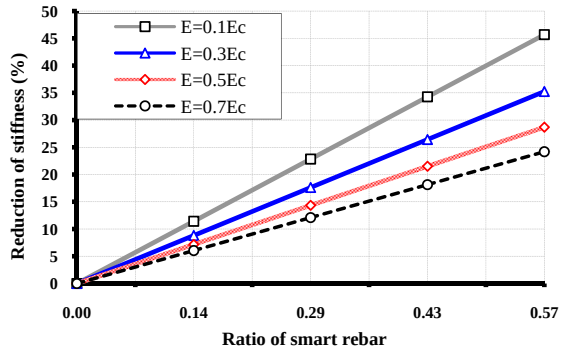

Fig. 13. Relationship between reduction of stiffness and ratio of smart rebar.

modulus to $0.7E_c$, the effect of both loading amplitude and reduction of residual displacement have disappeared and also all the curves fit well to each other.

6.3. Stiffness

Due to use of an elastic material with low elastic modulus instead of concrete, the neutral axis position falls on the geometrical center of the beam cross section. Therefore, both tension and compression conditions are symmetrical for all of the models in the beam cross-section. Since the section is symmetrical without considering any cracking, the tension and compression reinforcements yield simultaneously. Thus the lateral stiffness of the beam is divided in three different zones. Figure 12 presents the schematic diagram of the load-displacement relationship from the initial displacement to its maximum.

In zone OA, all materials have elastic behavior and the stiffness of the models obtained by using the strength of materials formula similar to section 4.3.

Table 7. Lateral stiffness of the models in linear area.

Concrete Young's Modulus	Ratio of Smart Rebar	Stiffness (KN/m)	Reduction of stiffness (%)
$0.1E_c$	0.00	2979.1	0.0
	0.14	2638.9	11.4
	0.29	2298.7	22.8
	0.43	1958.5	34.3
	0.57	1618.3	45.7
$0.3E_c$	0.00	3861.3	0.0
	0.14	3521.1	8.8
	0.29	3180.9	17.6
	0.43	2840.7	26.4
	0.57	2500.5	35.2
$0.5E_c$	0.00	4743.5	0.0
	0.14	4403.3	7.2
	0.29	4063.1	14.3
	0.43	3722.9	21.5
	0.57	3382.7	28.7
$0.7E_c$	0.00	5625.7	0.0
	0.14	5285.5	6.0
	0.29	4945.3	12.1
	0.43	4605.1	18.1
	0.57	4264.9	24.2

The lateral stiffness of the models in linear range is summarized in table 7. As seen in this table, smart rebar reduce stiffness of the beam. This is because Young's Modulus of SMA is much lower than that of steel reinforcement. Furthermore, for the models with the certain strength of concrete, the reduction of stiffness has been calculated as a percentage of stiffness of the model without SMA rebars. Figure 13 shows the reduction of stiffness as a percentage due to ratio of smart rebar. It can be observed that the more the strength of concrete increases, the less the effect of smart rebar on decreasing the lateral stiffness is.

After studying the lateral stiffness of the beam in elastic range, it can be investigated in inelastic area. In figure 12, steel rebars yield at point A and smart rebars yield at point B. Increase in the ratio of smart rebar increases the lateral stiffness in AB zone. This is due to elastic behavior of smart rebar in this zone.

Because of the fact that modulus of smart rebar is larger than that of steel after yielding and phase transition, increase in the ratio of smart rebar,

also slightly increases the lateral stiffness in BC zone.

7. Conclusions

The response of RC beams using smart rebars under static lateral loading is numerically studied using the finite element method. The 3-D model of the concrete beam has been generated by ANSYS software; SOLID85 and SOLID185 have been used for the modeling of concrete and longitudinal reinforcement, respectively.Based onstudy presented, the following conclusions are summarized:

(1) Replacing steel bars with SMA bars reduces the area of the hysteresis P-Ä curves.

(2) Using smart rebar reduces the residual displacement of the beams after lateral cyclic loading.

(3) Load-Displacement curve of the beam can be divided into 5 zones:
- Zone 1: Concrete has no cracks, and all materials have elastic behavior.
- Zone 2: Concrete has cracked and rebars have elastic behavior.
- Zone 3: Tensile steel bars yielded and remaining rebars (SMA & compression steel) still have elastic behavior.
- Zone 4: Compression steel bars yieldbut smart bars still have elastic behavior.
- Zone 5: Tensile smart bars yield in this zone.

(4) Increase in the ratio of smart rebar reduces lateral stiffness of the beam in zones 1, 2 and 3.

(5) Increase in the ratio of smart rebar slightly increases lateral stiffness of the beam in zones 4 and 5.

(6) Even though SMA reduces residual displacements in RC beams due to its recoverability, it reduces energy absorption capacity of the structure.

Acknowledgement

The authors are grateful to the center of Excellence in Structures and Earthquake Engineering at Sharif University of Technology for providing supports in conducting this investigation.

References

[1] Janke, A., Czaderski, C., Motavalli, M. and Ruth, J.:2005, Applications of shape memory alloys in civil engineering structures - Overview, limits and new ideas, Materials and Structures,38, 578-592.

[2] Song, G., Ma, N. and Li, H.N.:2006, Applications of shape memory alloys in civil structures.Engineering Structures, 28, 1266–1274.

[3] Duering, T.W., Melton, K.N., Stökel, D. andWayman C.M. (eds):1990, Engineering aspects of shape memory alloys. Butterworth-Heinemann(London),pp. 1-35.

[4] Khaloo, A.R., Aghl P.P. andEshghi, I.:2009, Applications of Shape Memory Alloys in Concrete Structures. 3rd International Conference on Concrete & Development (Tehran, Iran), pp. 123-132.

[5] Tamai, H. and Kitagawa, Y.: 2002, Pseudoelastic behavior of shape memory alloy wires and its application to seismic resistance member for building, Computational Materials Science, 25, 218–27.

[6] DesRoches, R. andDelemont, M.: 2002, Seismic retrofit of simply supported bridges using shape memory alloys, EngStruct., 24,325-332.

[7] Cardone, D., Dolce M.,Ponzo, F.C. and Coelho, E.:2004,Experimental behavior of R/C frames retrofitted with dissipating and re-centring braces, Journal of Earthquake Engineering, 8 (3), 361–396.

[8] Otero, K.: 2004, Intelligent reinforced concrete structures using shape memory alloys, M.S. thesis. Advisor: Dr. G. Song, University of Houston.

[9] Effendy, E., Liao, W.I., Song, G., Mo, Y.L. andLoh, C.H.: 2006, Seismic Behavior of Low-Rise Shear Walls with SMA Bars, ASCE, Earth & Space, 1-8.

[10] Janke, L.,Czaderski, C.,Motavalli, M. and Ruth, J.: 2005, Applications of shape memory alloys in civil engineering structures – Overview limits and new ideas, Materials and Structures, 38, 578-592.

[11] Buehler,W.J. and Wiley, R.C.:1965, Nickel-based alloys. US patent 3174851.

[12] Saiidi, M.S. and Wang, H.:2006, Exploratory Study of Seismic Response of Concrete Columns with Shape Memory Alloys Reinforcement. ACI Structural Journal, 103(3),436-443.

[13] Saiidi, M.S., Zadeh, M.S., Ayoub, C. andItani, A.:2007, Pilot study of behavior of concrete beams reinforced with shape memory alloys. J Mater Civil Eng, 19(6), 454-61.

[14] Li, H., Liu, Z.Q. andOu, J.P.:2006, Behavior of a simple concrete beam driven by shape memory alloy wires. Smart Materials and Structures, 15(4), 1039–46.

[15] Czaderski, C., Hahnebach, B. andMotavalli, M.:2006, RC beam with variable stiffness and strength. Construction and Building Materials, 20, 824–833.

[16] Willam, K.J. andWarnke, E.D.: 1975, Constitutive model for the triaxial behavior of concrete:Int. association for bridge and structural engineering (Bergamo,Italy).

[17] Auricchio, F. and Sacco, E.A.:1997, one dimensional superelastic model for shape memory alloys with different elastic properties between austenite and martensite. J.Non-Linear Mechanics, 32, 1101-1114.

[18] Auricchio, F.:1995, Shape memory alloys: Application, micromechanics, macromodeling and numerical simulations:Ph.D.dissertation University of California at Berkeley.

[19] ANSYS,Ansysuser manual revision 10.0, ANSYS,Inc.

[20] ACI 318-05, American Concrete Institute, Farmington hills, Michigan, 2005.